Article

Optimal Sizing of a Photovoltaic/Battery Energy Storage System to Supply Electric Substation Auxiliary Systems under Contingency

Ailton Gonçalves [1]**, Gustavo O. Cavalcanti** [1]**, Marcílio A. F. Feitosa** [1]🆔**, Roberto F. Dias Filho** [1]🆔**, Alex C. Pereira** [2]🆔**, Eduardo B. Jatobá** [2]🆔**, José Bione de Melo Filho** [2]**, Manoel H. N. Marinho** [1]🆔**, Attilio Converti** [3,]*🆔 **and Luis A. Gómez-Malagón** [1]🆔

[1] Postgraduate Program in Systems Engineering, Department of System Engineering,
     Polytechnic School of Pernambuco, University of Pernambuco, Recife 50720-001, PE, Brazil;
     ags3@poli.br (A.G.); gustavooc@poli.br (G.O.C.); marcilio@poli.br (M.A.F.F.); roberto.dias@upe.br (R.F.D.F.);
     marinho75@poli.br (M.H.N.M.); lagomezma@poli.br (L.A.G.-M.)
[2] São Francisco Hydroelectric Company (Chesf), Recife 50761-901, PE, Brazil; alexcp@chesf.com.br (A.C.P.);
     ejatoba@chesf.com.br (E.B.J.); jbionef@chesf.gov.br (J.B.d.M.F.)
[3] Department of Civil, Chemical and Environmental Engineering, Pole of Chemical Engineering,
     University of Genoa, Via Opera Pia 15, 16145 Genoa, Italy
*   Correspondence: converti@unige.it

Abstract: Electric substations (ESS) are important facilities that must operate even under contingency to guarantee the electrical system's performance. To achieve this goal, the Brazilian national electricity system operator establishes that alternating current (AC) auxiliary systems of ESS must have, at least, two power supplies, and in the case of failure of these sources, an emergency generator (EG) must at least supply energy to the essential loads. In order to improve the availability of auxiliary systems, a microgrid with other sources, such as photovoltaic (PV) systems and Battery Energy Storage Systems (BESS), can be an alternative. In this case, an economical optimization of the PV/BESS system must be addressed considering the costs associated with the installation and maintenance of equipment, and the gains from the credits generated by the photovoltaic system in the net metering scheme. In this paper, the size of the BESS system was determined to supply energy to the load of auxiliary systems of an ESS, as well as a PV system to achieve a null total cost. Furthermore, multi-objective optimization using the genetic algorithm technique was employed to optimize the size of the hybrid PV/BESS to minimize the investment cost and time when the demand was not met. Simulations under different scenarios of contingency were allowed to obtain the Pareto frontier for the optimal sizing of a PV/BESS system to supply energy to AC auxiliary systems in an ESS under contingency.

Keywords: auxiliary systems; battery management systems; microgrids; photovoltaic systems; substation

1. Introduction

Electric substations (ESS) represent the nodes of power systems. Constructively, they are facilities responsible for routing the flux of energy, under certain voltage levels, throughout the electric grid. To guarantee the operation of the substation, auxiliary systems are connected to alternating current (AC) and direct current (DC) busbars and installed to enable the functions of monitoring, protection, communication, lighting, and the main maneuvering of circuit breakers, among others. Due to their importance, auxiliary systems must be supplied counting on backup energy sources. For the Brazilian electrical power system, the electric system operator establishes the requirements to supply energy to the AC and DC busbars. In particular, the grid procedure for the minimum requirements for AC auxiliary systems establishes that they must have two independent power supplies such that, in the event of a failure in the main source, loads must be automatically transferred to

the other power supply and, in case of outage of both, the AC auxiliary systems must have an emergency generator (EG) set with automatic start and the capacity for supplying the substation's essential loads. DC auxiliary systems must have a stationary battery storage system able to supply energy, in the case of shutdown of the AC busbar, for at least 5 h for the protection and Supervisory Control and Data Acquisition (SCADA) system, and at least 10 h for the telecom system [1].

Due to the critical function of the ESS auxiliary systems, they must be ready to operate under contingencies. However, the operation of the backup power supply systems is expensive and not environmentally friendly in the case of EG's operation. Other alternatives to supply energy to the AC busbar must be explored to mitigate these problems and increase the availability of auxiliary systems. At this point, due to the technological maturity of photovoltaic systems, this technology is a candidate to supply energy to auxiliary systems under contingencies and contribute to the decarbonization of the power sector. However, due to the intermittency of solar energy, it is necessary to integrate the photovoltaic system with a storage system to guarantee a constant energy supply in the islanded operation mode. This integration constitutes an islandable microgrid, which in Brazil must be sized to supply energy according to the requirements of the National Electricity System Operator (ESO) (Operador Nacional do Sistema—ONS, its acronym in Portuguese). This means that, under contingency, a photovoltaic (PV) and a Battery Energy Storage System (BESS) must supply power to the auxiliary systems for at least 10 h. Therefore, the economical optimal sizing of a hybrid PV/BESS to supply energy to auxiliary systems is a challenge due to the trade-off between the costs associated with the installation and maintenance of equipment and the gain due to credits in the net-metering mode operation of a PV system. Additionally, if an EG is considered during the operation under contingency, the environmental impact must be taken into account.

The optimal size of a PV/battery system implies the correct description of these energy sources. The optimal exploration of intermittent energy sources, such as photovoltaic or wind power systems, depends on the correct predictability of the energy resource. As indicated by the Energy Research Company (Empresa de Pesquisa Energetica—EPE, its acronym in Portuguese), measurements of the solar resource for at least 12 months are needed to estimate the energy production of a place for a photovoltaic plant [2]. The estimation of the in situ energy production is a common procedure in the photovoltaic industry; however, in some cases, it is not possible, and the energy production is estimated from available data in the solar resource maps or solar monitoring stations installed closer to the local. The analysis of irradiance measurement data is very important to predict the behavior of the PV system. For this purpose, physical, statistical, and empirical models are well-reported in the literature to fit experimental data [3,4]. However, recent computational techniques have been shown to be useful to obtain better results compared to the traditional methods [5,6].

On the other hand, the correct choice of battery technology is a challenge to fulfill the load requirements. According to the application, batteries must be chosen to take into account the power density, energy, response time, and efficiency, among other variables [7]. For power applications, lead–acid (LA) and lithium-ion (Li-ion) batteries are the most reported in the literature [8,9]. Different aspects can be compared between them. Typically, LA batteries have better performance in terms of cost, recycling rate, and safety, while Li-ion ones show a high depth of discharge and efficiency, are considered more environmentally friendly, and are significantly lighter and more compact [10]. So, the correct choice of the technology will depend on the application. In the case of a BESS, to supply energy to the ESS auxiliary systems, a mix of battery technologies have been proposed [11]. Due to the strategic relevance in the energy storage industry, the development of new ways to overcome the problems of these technologies and the proposal of new storage systems are considered hot research topics in energy [12].

Considering the previous aspects related to the solar resource and battery technology, the optimal size of PV/battery or PV/diesel/battery can be analyzed, for example,

considering (i) the objectives that should be maximized/minimized such as costs, CO_2 emissions, availability [13,14]; (ii) the assumptions considered in the model, such as the lifetime and degradation of the batteries [15,16], tariff schemes [17], load profiles [18]; and (iii) computational techniques employed in the optimization process such as genetic algorithms [19,20], stochastic programming models [21], Mixed-Integer Linear Programming (MILP) [22], and teaching- and learning-based optimization algorithms [23], among others. Another important variable to be considered in these systems is the connection mode. In the case of a grid-connected system, different examples are available in the literature showing energy management strategies to supply optimally the energy sources [24–29], even under daily blackouts, contingencies [30,31], or random contingencies due to extreme climate events or other causes. In all these cases, efforts are addressed to optimize the energy flow in power distribution networks to increase resilience [32–34].

Despite the wide discussion about the sizing of hybrid systems considering different variables and techniques, there are few reports available in the literature discussing the sizing of a grid-connected hybrid system under contingencies with well-established duration time given by regulatory policies as in the case of ESS auxiliary systems [11,35]. For example, the optimal size of the PV/BESS was determined by minimizing the total cost of the investment using Monte Carlo simulations to assess the variability of the solar resource and the uncertainties of contingencies [35]. Hybrid Optimization of Multiple Energy Resources (HOMER) software was also used to size the PV/BESS to meet the demand [11,36]. Additionally, for this kind of system, the dynamic response of the electrical variables under different connection scenarios was analyzed [37,38].

In this paper, we present a case study of an ESS in which there are constraints on the independence of the energy supply lines to the ancillary sources as established by the ESO. Then, the main contribution is sizing (power) the PV/BESS to comply with the ESO requirements and increase the substation availability, not only to supply energy in the case of a large contingency (designed for at least 10 h), but also to use the BESS Energy Management System (EMS), which will contribute to decreasing the number of shutdowns associated with automatic connection in the case of contingency. For the National Interconnected System (Sistema Interligado Nacional-SIN in Portuguese), this type of fault contributes to 50% of the total faults associated with the electric substation auxiliary system [39]. In particular, this study considers only the BESS to supply energy to the load and a PV system to compensate for the investments in order to obtain a null total cost. Additionally, the sizing of the hybrid PV/BESS is obtained by minimizing the unavailability and the investment cost using multi-objective techniques considering the ESO requirements, solar resource variability, contingencies, and load profile.

2. Materials and Methods

2.1. Case Study

The Teotônio Vilela substation, also known as Messias ESS, is located in Messias-Brazil (09°23′00″ S; 35°50′30″ W) and is responsible for lowering voltage from 500 to 230 kV and switching the 500 kV transmission line coming from the Xingó Hydroelectric Power Plant to the Suape II substation. It has a breaker-and-a-half configuration in the 500 kV sector and a double busbar with four switches in the 230 kV one. In its final configuration, the ESS will have a total installed capacity of 1800 MVA by 2023. The Messias ESS is responsible for supplying the State of Alagoas, including some industrial customers, and it also makes up the main axis serving the eastern area of the northeast region of Brazil. The ESS has auxiliary systems responsible for the SCADA, protection, and telecommunication systems.

According to the ESO, auxiliary systems must be supplied by two independent AC sources, such that, in the case of a fault in the main power supply, the first AC source can be replaced by the second one. In the case of faults in both power supply sources, the system must have at least one EG, as shown in Figure 1. In the Messias ESS, the main and auxiliary power supply sources come from the same company (Equatorial Energy Alagoas, Brazil)

supplying energy at 69 kV and 13.8 kV, respectively, and the backup system has two EGs of 225 kVA and 600 kVA connected directly to the AC 440 V busbar.
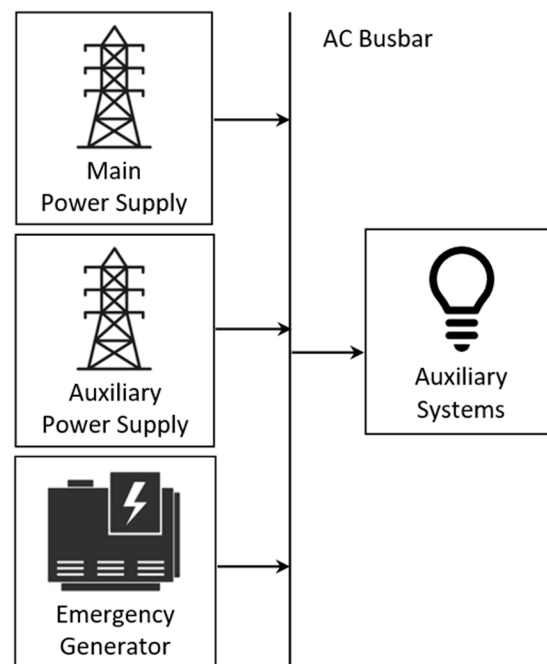

Figure 1. Scheme of the alternating current (AC) busbar supplied by the main grid, auxiliary power supply, and emergency generator.

It is important to note that, in the Messias ESS, the main and auxiliary power supply lines are not independent, as requested by the ESO. The origin of this non-compliance dates to the Messias's construction, about 25 years ago. Since then, the ESO changed many of its requirements. As a result, any retrofit event in the ESS will contribute to fulfilling the current ESO requirements.

The load profile of the auxiliary systems was obtained by measuring the apparent power using a power quality and energy analyzer (model 435, Fluke, Everett, WA, USA) connected to the AC busbar. Measurements were taken in July 2022 and analyzed according to the procedures of electric energy distribution [40]. The representative load profile of the Messias ESS was obtained by taking the average of the mean apparent power measurements. The average value and its standard deviation are shown in Figure 2. Accordingly, the maximum power is required at night in the interval from 18:00 to 6:00 due to illumination loads.
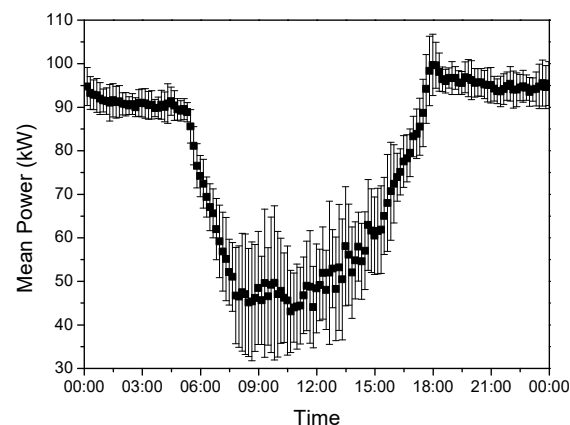

Figure 2. Load profile curve of the Messias ESS showing the average value and standard deviation of the total apparent power consumed by auxiliary systems.

2.2. Hybrid PV/BESS System

Considering that the operation of the Messias substation must be continuous even in the presence of a contingency, to comply with the current legislation about the independency of the auxiliary power supplies, improve the availability of the system, and avoid the operation and environmental issues due to EG operation, an extra backup supply source based in the integration of a PV plant and a BESS is proposed, as shown in Figure 3.
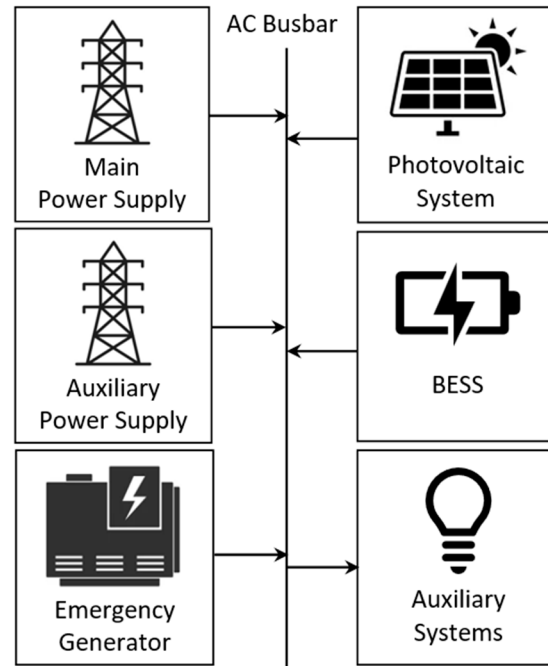

Figure 3. Scheme of the AC busbar supplied by the main grid, auxiliary power supply, emergency generator, and a PV/BESS.

According to Figure 3, different scenarios of scheduling the power sources can be supposed in the case of contingency, such as using each backup system independently or simultaneously. However, in order to size the PV/BESS system, only the scenario where the auxiliary systems are supplied by the PV/BESS system is taken into account. Consequently, two cases are possible: the one considering only the BESS and the other considering its integration with the PV system to supply energy to auxiliary systems.

2.3. Problem Statement

The optimal size of the PV/BESS is obtained through the analysis of total costs and investments involved in the project, as well as the level of availability to supply power to the load. So, the optimal size of the BESS and the PV/BESS can be thought of as a multi-objective problem of investment minimization and availability maximization, subjected to the constraint related to the system energy balance, such that the total energy generated should not exceed the demand, avoiding system oversizing and cost increase. In this case, the constraint is given by:

$$E_{BESS}(t) + E_{PV}(t) \leq E_D(t) \tag{1}$$

where $E_{BESS}(t)$, $E_{PV}(t)$, and $E_D(t)$ are the energies supplied by the BESS, which are supplied by the PV system and required by the load, respectively.

2.4. Economic Modelling

The economic analysis for the PV/BESS takes into account the costs associated with the purchase of equipment, the operation and maintenance (O&M), and the profit coming from energy generated by the PV system.

Considering that the equipment is bought at the beginning of the operation, the investment costs, due to the purchase and installation of BESS and PV systems, are given by:

$$I_{PV/BESS} = P_{PV} c_{PV} + P_{BESS} c_{BESS} \tag{2}$$

where $I_{PV/BESS}$ is the investment in the PV/BESS expressed in Brazilian Reals (BRLs), P_{PV} and c_{PV} are the power (kW) and cost (BRL/kWp) of the PV system, $P_{BESS,}$ and c_{BESS} are the storage capacity (kWh) and cost (BRL/kWh) of the BESS.

The present value of the O&M costs ($C_{O\&M}$) is calculated as a percentage of the investments during the equipment lifespan (*n*) at an interest rate (*i*) as:

$$C_{O\&M} = \sum_{n=1}^{N} \frac{P_{PV} \, c_{PV} \, c_{O\&M,PV} + P_{BESS} \, c_{BESS} \, c_{O\&M,BESS}}{(1+i)^n} \tag{3}$$

where $c_{O\&M,PV}$ and $c_{O\&M,BESS}$ are the fractions of investment annually spent in O&M of the PV system and BESS, respectively.

The total investment of the PV/BESS ($TI_{PV/BESS}$) is then given by:

$$TI_{PV/BESS} = I_{PV/BESS} + C_{O\&M} \tag{4}$$

Furthermore, the operation of the PV system will generate credits in the net-metering scheme that can be consumed according to the tariff applied during the generation; therefore, the gain of the PV system ($Profit_{PV}$) is given by:

$$Profit_{PV} = \sum_{1=1}^{N} \frac{T_1 \, CE_{PVi}}{(1+i)^n} \tag{5}$$

where T_1 is the off-peak tariff and CE_{PVi} are the credits obtained due to the injected energy into the grid.

These credits are given by the difference between the credits coming from the PV system generation (CE_{PV}) and the equivalent credits consumed by the load taking into account the peak/off-peak tariff ($CE_{equivalentPV}$) [41] according to the following equations:

$$CE_{PVi} = CE_{PV} - CE_{equivalent \, PV} \tag{6}$$

$$CE_{PV} = \int \eta_{PV} \, I \, A_{PV} \, dt \tag{7}$$

$$CE_{equivalent \, PV} = \int_{off-peak} P_D dt + T_2 \int_{peak} P_D dt \tag{8}$$

where η_{PV} and A_{PV} are the efficiency and area of the PV system, I is the solar irradiance (W/m^2), T_2 is the peak/off-peak tariff ratio, t is the time, and P_D is the load profile given in Figure 2.

Then, the total cost (*TC*) is given by the difference between profit and investment:

$$TC = Profit_{PV} - TI_{PV/BESS} \tag{9}$$

2.5. Technical Modelling

The technical analysis involves the determination of the availability index (*A*), which is defined as the fraction of time when energy is available to supply the load, according to the following equation:

$$A = 1 - \frac{t_{DNM}}{t_D} \tag{10}$$

where t_{DNM} is the time when the demand is not met and t_D is the time when the demand must be supplied.

In continuous operation, t_D is equal to 8760 h per year, and t_{DNM} is zero when the energy delivered by the sources is enough to cope with the demand. Therefore, the availability can be expressed using A or t_{DNM}.

Due to the temporal behavior of the solar radiation, contingencies, and the discharge/charge process of batteries, the Transient System Simulation Tool (TRNSYS) software package (University of Wisconsin, Madison, WI, USA) was used to model the physical response of the system and to obtain the availability index [42]. This software is widely used to model PV systems, batteries, and other devices for optimization purposes [43–45]. The TRNSYS information flow diagram for the PV/BESS is shown in Figure 4. The Type 15-TMY3 component is employed for weather data reading and processing from a Meteonorm file. Meteonorm software (Meteotest, Bern, Switzerland) allows access to the historical time series of irradiation. These data are collected by the Type 103b component to model the electrical response of a PV system. The Type 47a component models a battery storage system specifying the temporal response of the battery state of charge given the rate of charge or discharge. The Type 14 h component has the load profile. The model of the PV/BESS is integrated with an open-source and multi-objective optimization software written in Python to run the optimization algorithm using the Pymoo library [46].
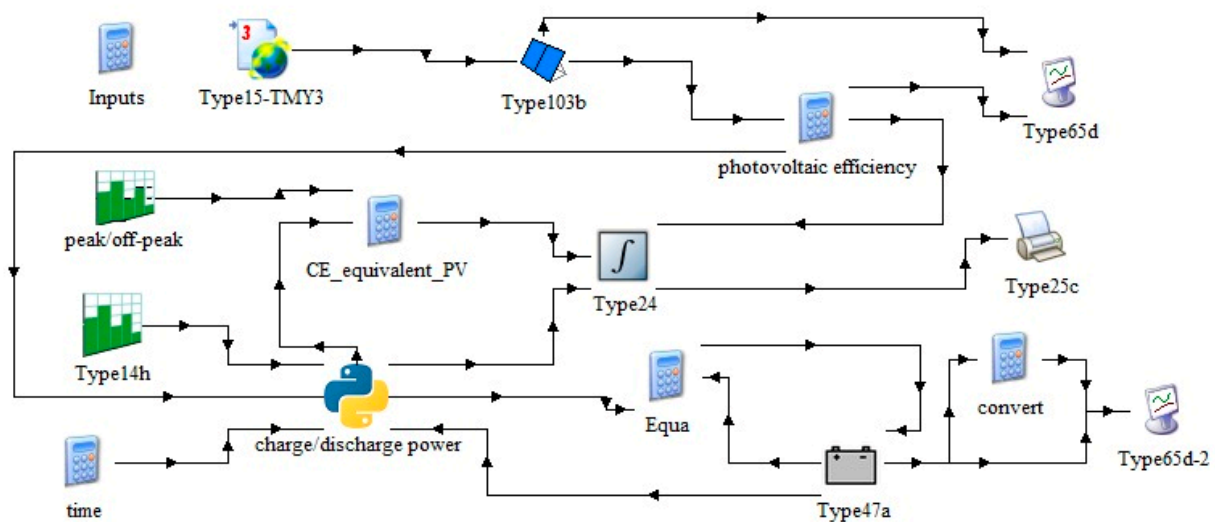

Figure 4. TRNSYS information flow diagram to simulate the PV/BESS coupled with Python software.

2.6. Optimization Process

Investments in the PV/BESS contribute to increasing the availability index. Without investment, the system will be unavailable during contingency, and increasing the investments the value of A will increase to its maximum value ($A = 1$). At this point, if the investments are increased, the value of A will not change. As the $TI_{PV/BESS}$ is a mix of investments in the PV system and the BESS, there is a set of decision variables (P_{PV} and P_{BESS}) that give the lowest value of the investment and maximum value of A. This is a multi-objective problem where the optimal decision must be taken by the decision maker. Then, this problem can be classified as an a posteriori optimization problem [47,48]. Different algorithms are available to solve this kind of problem. Normal Boundary Intersection (NBI), Normal Constraint (NC), and Direct Search Domain (DSD) are examples of mathematical programming, and the Multi-Objective Genetic Algorithm (MOGA), Multi-Objective Particle Swarm Optimization (MOPSO), and Simulated Annealing (SA) are examples of evolutionary algorithms [49]. The MOGA is a metaheuristic optimization algorithm that emulates natural selection. In particular, the Non-dominated Sorting Genetic Algorithm II (NSGA-II) was employed to solve the proposed multi-objective problem, thanks to its ability to solve them by classifying the solutions according to the dominance degree [50]. This characteristic is explored in the literature in the study of microgrids [51–57]. The flowchart representing the GA algorithm is shown in Figure 5.
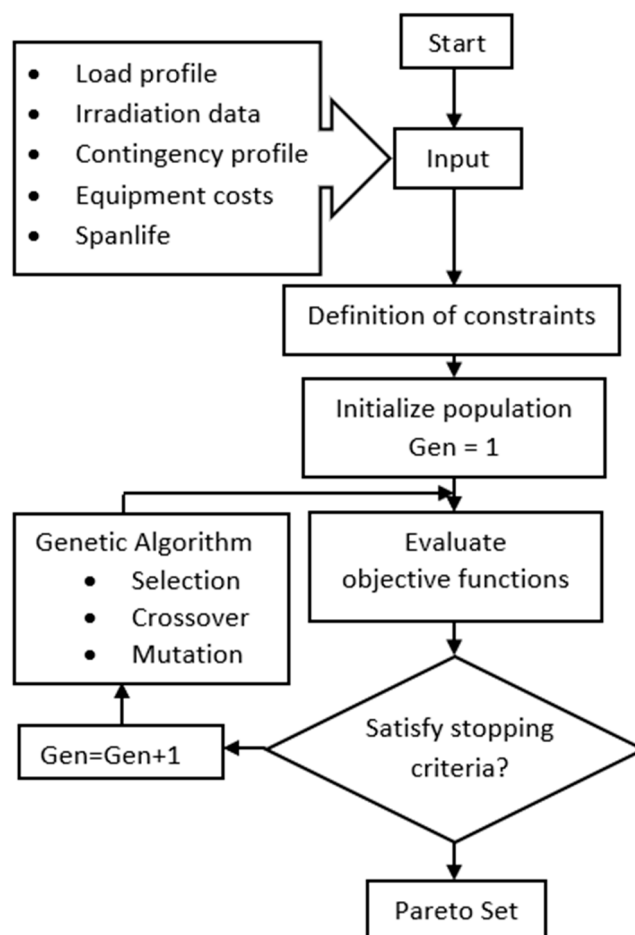
Figure 5. Genetic algorithm flowchart for optimal PV/BESS.

According to this figure, the algorithm starts loading the input data and defining the constraints about energy balance and others related to the nature of variables (e.g., non-negative values and maximum values of power and efficiency). The algorithm initializes the population by choosing a random value of the decision variables (P_{PV} and P_{BESS}) to evaluate the objective functions ($TI_{PV/BESS}$ and A). If the stopping criteria given by the maximum number of generations and the convergence tolerance are not satisfied, the GA creates a new population through the selection, crossover, and mutation process to be tested in the objective functions until achieving the convergence criteria. Finally, the population that defines the Pareto frontier, which is a set of non-dominated solutions, is reported. In the algorithm, 100 search agents were employed, and the stopping criteria were the maximum number of generations and the generation distance, which were set at 200 and 10^{-2}, respectively. After running the algorithm, the Pareto frontier was obtained after 10 generations.

3. Results

3.1. Scenario 1: Only BESS

In this scenario, the energy supply to the auxiliary systems is considered to be provided only by the BESS, whose size is determined considering the load profile given in Figure 2 and different ranges and durations for the contingency. Depending on the BESS size, the availability index changes. It is observed that the availability index is equal to the unity when the BESS's capacity is greater than 700 kWh and varies according to the contingency duration (10 or 12 h), whether it happens during the day (e.g., 6:00–18:00) or at night (e.g., 18:00–6:00), as shown in Figure 6.
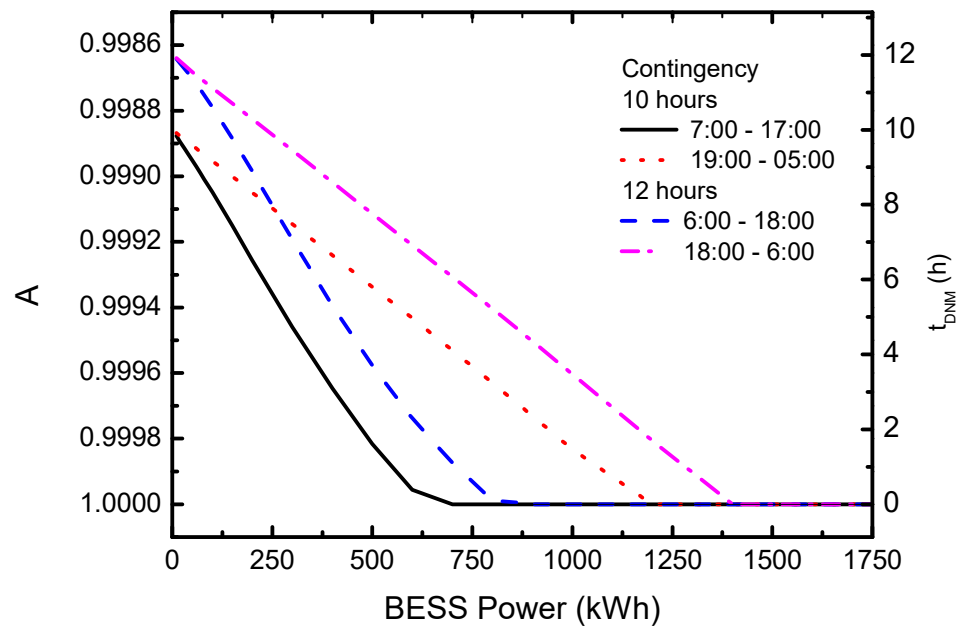
Figure 6. Availability index of BESS power for different contingencies.

To exemplify the BESS's behavior, the temporal response of the BESS, with capacities of 500 and 1000 kWh, considering contingencies between 7:00 and 17:00 and from 19:00 to 5:00, are given in Figure 7. It is observed that for the 500 kWh BESS capacity, there is a time interval where the BESS cannot supply energy to the load because it is in the lowest state of charge (*SOC*), defined as 20% of its capacity (100 kWh). Comparing the time intervals where the BESS is at its minimum value, the interval during the day is lower than that at night. This is due to the load profile, also shown in Figure 7, which shows lower values during the day than at night. In contrast, for the 1000 kWh BESS capacity, the BESS can supply all energy required by the load because the time interval at the minimum state of charge (200 kWh) was zero during the day and 1.5 h at night. It is important to note that these results were obtained considering one contingency per year. As reported by the Brazilian Electricity Regulatory Agency (Agência Nacional de Energia Elétrica—ANEEL in Portuguese), in 2017 and 2018, only four events per year led to the Brazilian electric system being recomposed in more than one hour [39]. Then, increasing the number of contingencies, the availability index decreases, although the BESS power to supply all energy to the load is the same, as shown in Figure 6.
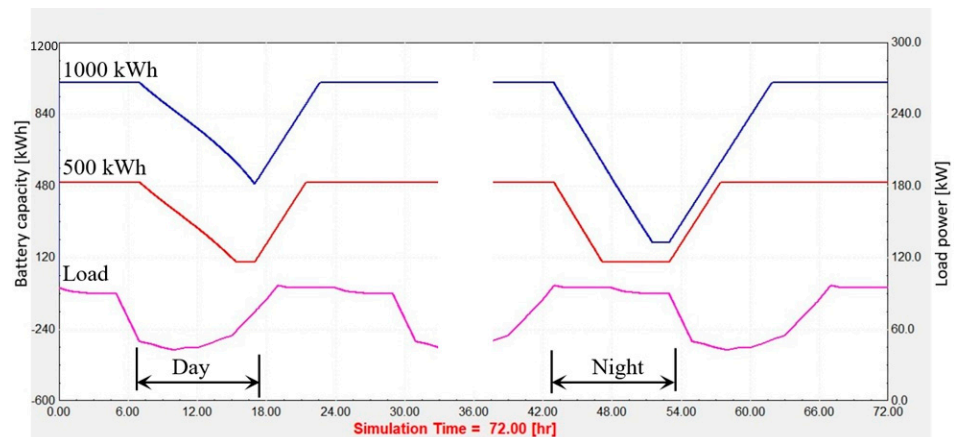

Figure 7. Temporal response of 1000 and 500 kWh batteries (blue and red lines) and the load profile (magenta line).

3.2. Scenario 2: PV/BESS System

In this scenario, the power of the PV system able to compensate for the BESS investment, which occurs when *TC* is zero, was obtained for the lowest BESS capacity, ensuring an availability index of one (Figure 6). The results for the *TC* are shown in Figure 8 and were determined using the values given in Table 1.
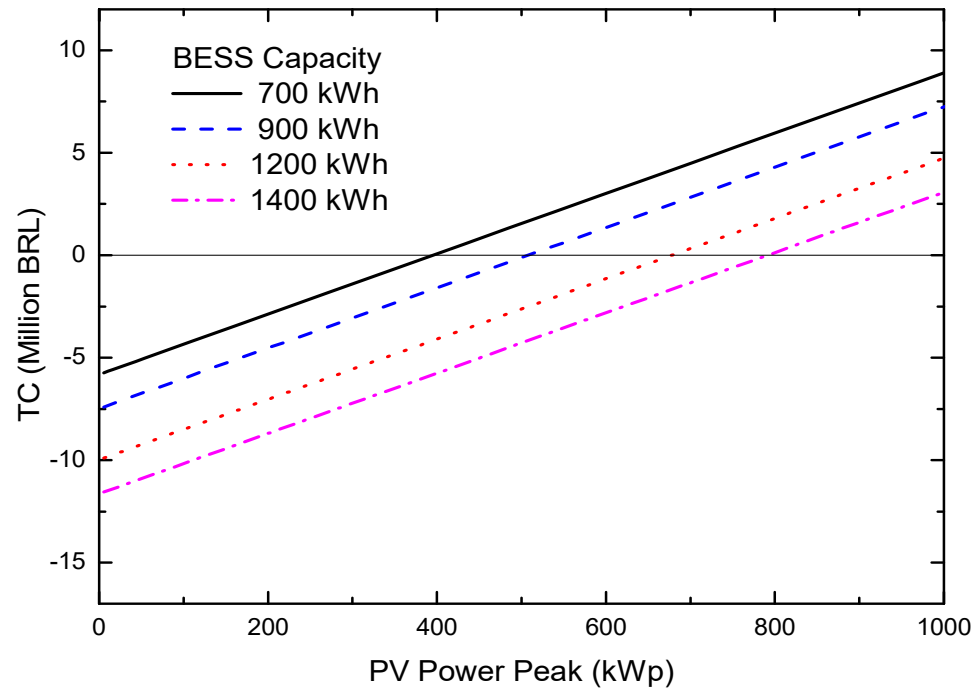

Figure 8. Total cost of a PV/BESS system versuss PV power considering the BESS capacity to obtain an available index of one. For comparison, 1 USD = 5.1 BRL.

Table 1. Variables employed in the economic analysis.

Variable	Value	Reference
n	20 years	[35]
i	6%	[35]
c_{PV}	4302.94 BRL/kWp	[11]
c_{BESS}	5945.10 BRL/kWh	[11]
$c_{O\&M, PV}$	1.0%	[35]
$c_{O\&M, BESS}$	2.5%	[58]
T_1 *	0.347 BRL/kWh	[59]
T_2 **	1.44	[59]

* Tariff includes other Brazilian taxes: PIS, ICMS, and CONFINS. ** The tariff for the Messias ESS belongs to group A, subgroup A3, seasonal blue.

It can be seen in this figure that without the PV system, *TC* is negative because only the investment in the BESS was taken into account. Increasing the PV power, *TC* increases, taking into account the investments of the PV system and the profits deriving from the credits obtained from the injected energy.

For null *TC*, the PV powers of 395, 505, 680, and 790 kW were determined for BESS capacities of 700, 900, 1200, and 1400 kWh, respectively. Compared with the results in Figure 7, the temporal responses of a PV/BESS system with a PV power of 16.2 and 108 kWp are shown in Figures 9 and 10, respectively.
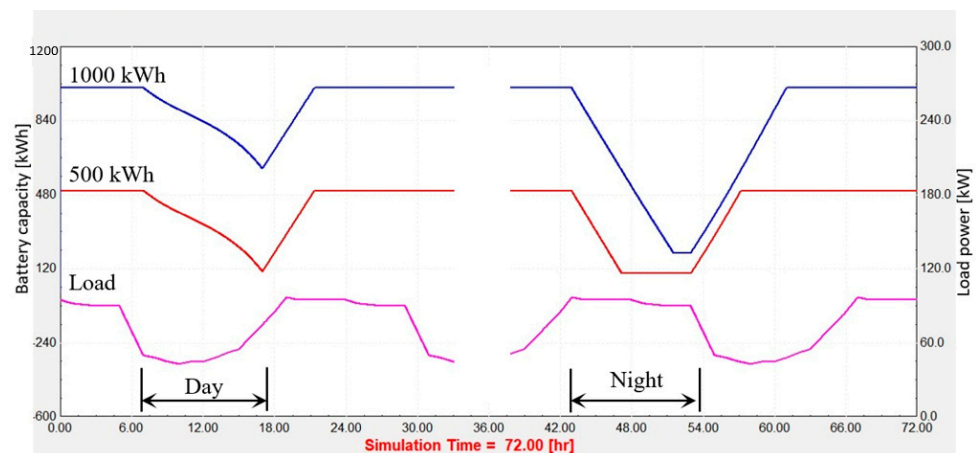
Figure 9. Temporal response of 1000 and 500 kWh batteries (blue and red lines) and the load profile (magenta line) connected with a 16.2 kWp PV system.
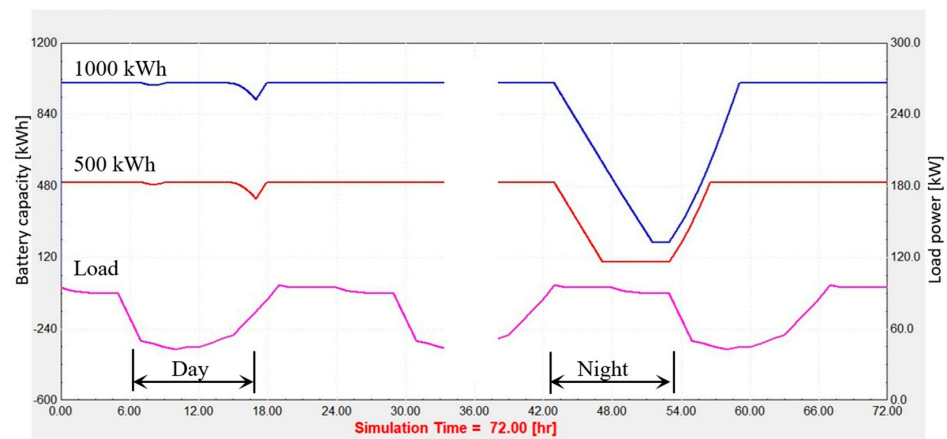

Figure 10. Temporal response of 1000 and 500 kWh batteries (blue and red lines) and the load profile (magenta line) connected with a 108 kWp PV system.

Figure 9 shows that during the day, the energy supplied by the PV system contributes to eliminating the unavailability by increasing the BESS *SOC* at the end of the contingency. By increasing the PV power to 108 kWp (Figure 10), the PV system is responsible for the supply of most of the energy to the load, with only a little BESS contribution. Moreover, as expected, at night, the BESS profile is kept the same because the contribution of the PV system is almost null.

3.3. Scenario 3: Optimized PV/BESS System

In this scenario, the objectives are to maximize A (minimize t_{DNM}) and minimize the investment. As the objectives are opposites, the solution to this problem consists of finding a set of decision variables that define the Pareto frontier. Frontiers were obtained considering a contingency of 10 h during the day (7:00–17:00) or at night (19:00–5:00).

The Pareto frontier for the contingency during the day (Figure 11) clearly shows the conflict of objectives, i.e., in the absence of investment, the time with demand not met is maximum (10 h), while increasing the investment decreases it until $t_{DNM} = 0$. In this case, the investment is about BRL 1.06 million. As the contingency was considered during the day (7:00–17:00), a large contribution of the PV system is expected to reduce t_{DNM}. However, a little part of the demand must be supplied by the BESS at the beginning and the end of the day, when solar radiation is low. The relationship between *TC* and the investment is shown in Figure 12. Due to the initial investment in the BESS, the first point of the *TC* curve is negative, but as the PV system increased, the profit generated from the

injected energy to the grid contributes to obtaining positive values of *TC*. Therefore, the best pair of PV power and BESS capacity minimizes t_{DNM} until a BRL 0.4 million investment is obtained, considering a fixed low BESS capacity and increasing the PV power (3D bar graph in Figure 13). Using this strategy, t_{DNM} is reduced to about 2 h and then zero by increasing the BESS capacity with a little change in the PV power. Then, a *TC* reduction due to the increase in expenses for equipment acquisition is expected. The best pair ensuring t_{DNM} = 0 and minimum investment are a PV power of 135 kWp and a BESS capacity of 80 kWh. Increasing the investments, there are other solutions capable of ensuring the objective of zero hours for the demand not met; however, they can increase or decrease the *TC* depending on the size of the PV/BESS system. Increasing the size of the PV/BESS system beyond the point of lowest investment, the best solution for ensuring a null total cost is a PV power of 167 kWp and 250 kWh with an investment of BRL 2.2 million.
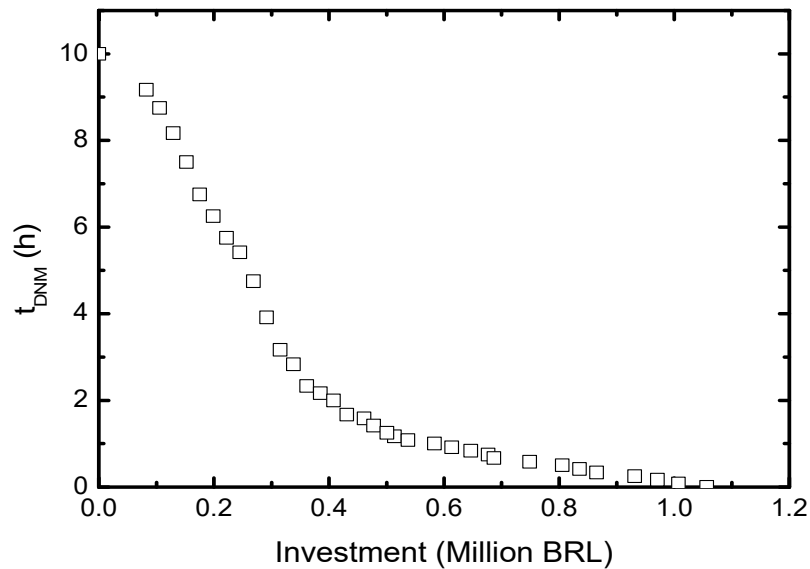

Figure 11. Best results that minimize the time when the demand is not met (t_{DNM}) and the investment (Pareto frontier) for a contingency during the day.
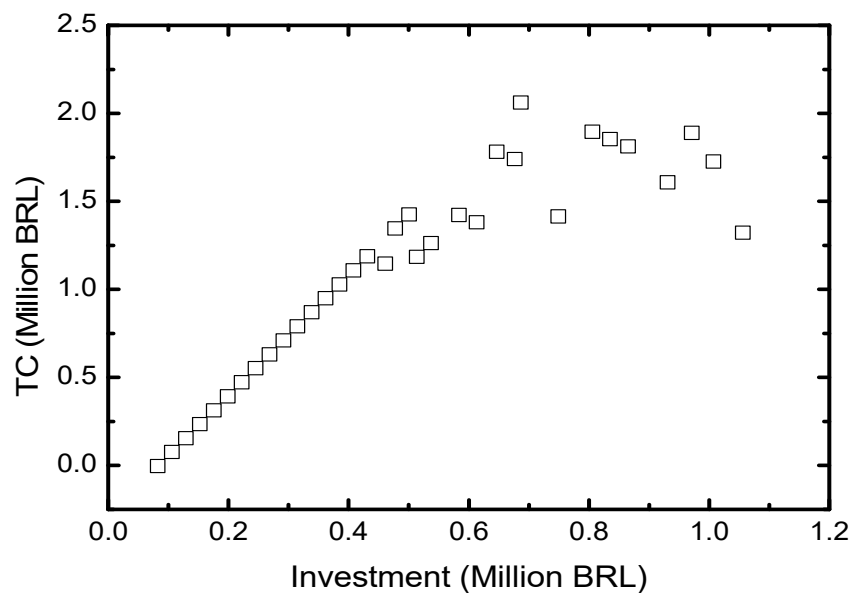

Figure 12. Total cost (*TC*) versus the investment for the scenario of contingency during the day. For comparison 1 USD = 5.1 BRL.
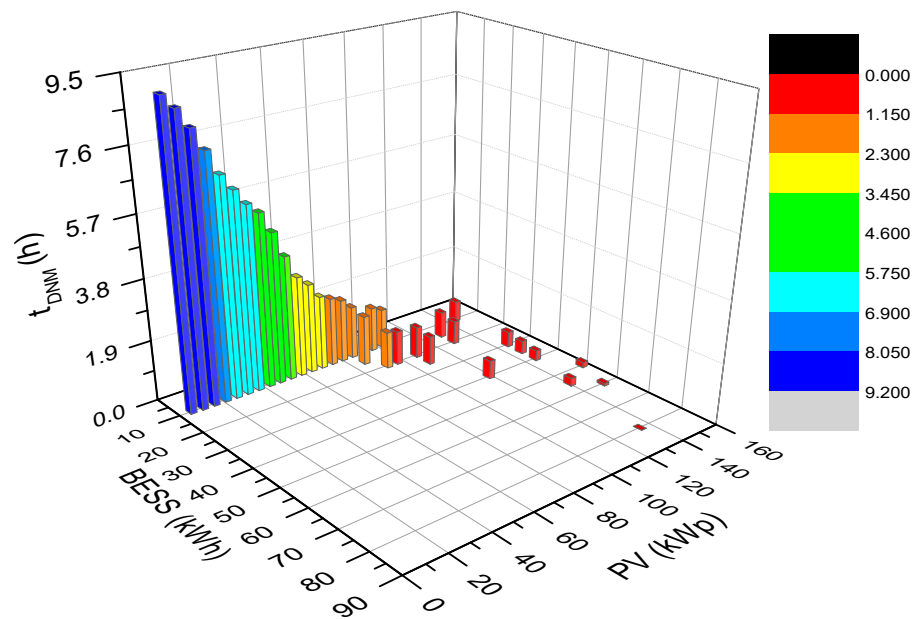
Figure 13. Simultaneous influence of PV power and BESS capacity on the time when the demand is not met (t_{DNM}).

Even though the Pareto frontier for a contingency at night (Figure 14) shows the same conflict of objectives, the relation between t_{DNM} and the investment is almost linear, and $t_{DNM} = 0$ is achieved for about BRL 7.16 million. In this scenario, it is expected that the contribution of a PV system shall be null, which is observed in Figure 15, which illustrates the influence of the investment on the total cost. As the investment is increased by the acquisition of the BESS, the total cost becomes more negative, showing a linear trend, which means that all investments are in BESS and not in PV systems. In the case of zero hours for the demand not met, investments in BESS greater than BRL 7.16 million also give zero t_{DNM}; however, these solutions do not contain one that represents the minimum investment and contributes to decreasing the total cost. Considering that it is necessary for a long number of charge/discharge processes to achieve the failure of the BESS during its lifespan, the obtained results are valid to attend to the number expected of contingencies per year [39].
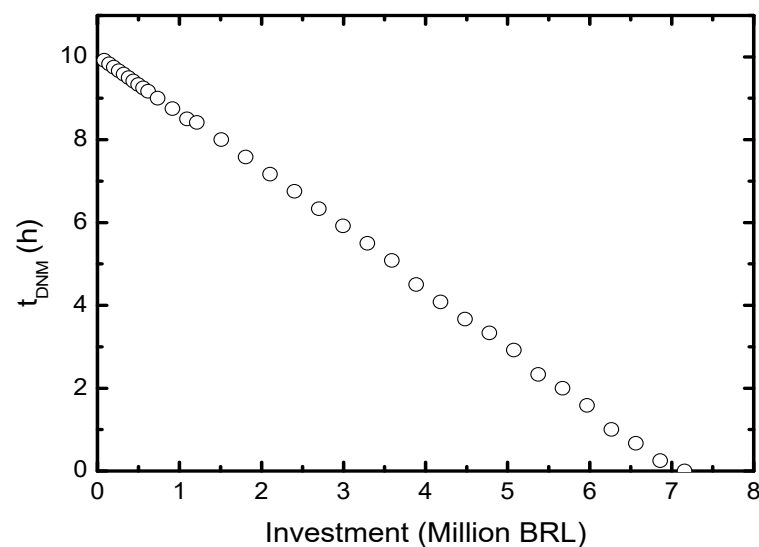

Figure 14. Best results that minimize t_{DNM} and investment (Pareto frontier) for a contingency of 10 h at night.
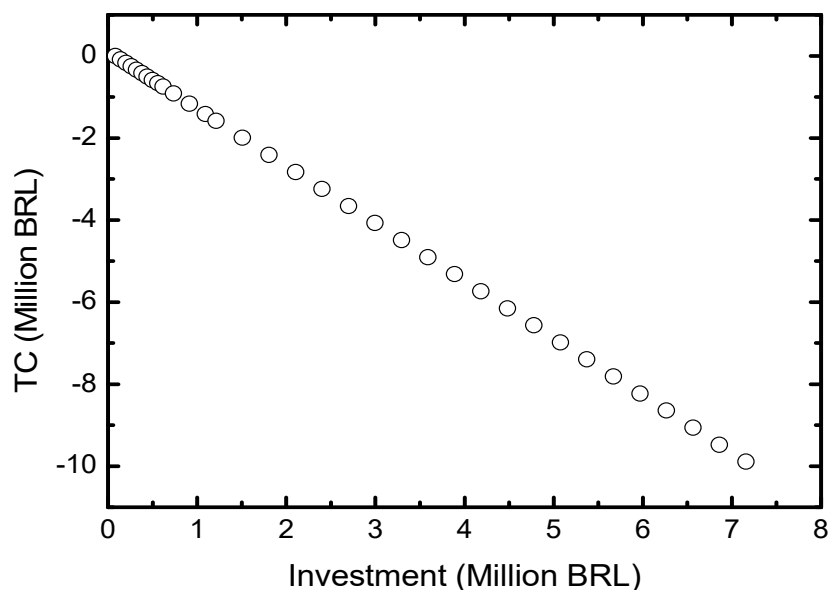
Figure 15. Total cost versus investment for a contingency scenario at night.

4. Conclusions

Hybrid systems using renewable energy sources and storage systems are alternatives to supply energy to auxiliary systems of electric substations (ESS), even under contingencies.

For the studied scenarios, depending on the contingency time, PV systems can give a strong contribution during the day and are null at night. In contrast, during a contingency at night, only the BESS can supply energy to the load. These results contribute to understanding how to schedule the supply of backup energy sources to optimize the lifetime of the equipment and the economical operation.

When only installing a BESS system, the total cost is negative. The role played by the PV system in total cost is to increase it such that it can be sized to achieve a total cost of zero. This means that the investments are paid by the credits obtained by the injection of energy into the grid by the PV system.

The multi-objective optimization of economic and technical variables showed that it is viable to introduce PV/BESS systems to supply energy to auxiliary systems in ESS. The use of PV/BESS systems can fulfill the requirements of the Brazilian National Electricity System Operator for ESS, increasing its availability under contingency.

The presented methodology can be used for investment analysis considering other variables such as the location of the ESS, its duration, frequency, and timetable of the contingency.

Author Contributions: Conceptualization, R.F.D.F., A.C.P. and L.A.G.-M.; methodology, A.G. and L.A.G.-M.; software, A.G.; validation, A.G., G.O.C., M.A.F.F., R.F.D.F., A.C.P., E.B.J., J.B.d.M.F., M.H.N.M., A.C. and L.A.G.-M.; formal analysis, A.G. and L.A.G.-M.; investigation, A.G., R.F.D.F., A.C.P. and L.A.G.-M.; writing—original draft preparation, A.G., G.O.C., M.A.F.F., R.F.D.F., A.C.P. and L.A.G.-M.; writing—review and editing, A.G., G.O.C., M.A.F.F., R.F.D.F., A.C.P., M.H.N.M., A.C. and L.A.G.-M.; visualization, A.G., G.O.C., M.A.F.F., R.F.D.F., A.C.P., E.B.J., J.B.d.M.F., M.H.N.M., A.C. and L.A.G.-M.; supervision, L.A.G.-M. All authors have read and agreed to the published version of the manuscript.

References

1. ONS—Operador Nacional do Sistema Elétrico. Requisitos Mínimos Para Subestações e Seus Equipamentos. Submódulo 2.6. 2022. Available online: https://apps08.ons.org.br/ONS.Sintegre.Proxy/ecmprsite/ecmfragmentsdocuments/Subm%C3%B3dulo%202.6-RQ_2021.08.docx_261430f7-8a33-4963-a75b-26578bef0c0f.pdf (accessed on 6 June 2023).
2. Empresa de Pesquisa Energética. Instruções Para Solicitação de Cadastramento e Habilitação Técnica com Vistas à Participação nos Leilões de Energia Elétrica [Internet]. Instruções Para Solicitação de Cadastramento e Habilitação Técnica com vistas à Participação nos Leilões de Energia Elétrica. N. EPE-DEE-RE-065/2013-R8. 2021. Available online: https://www.epe.gov.br/sites-pt/leiloes-de-energia/Documents/EPE-DEE-RE-065_2013_R8_UFV.pdf (accessed on 6 June 2023).
3. Beckman, W.A.; Blair, N.; Duffie, J.A. *Solar Engineering of Thermal Processes, Photovoltaics and Wind*, 5th ed.; John Wiley & Sons, Inc.: Hoboken, NJ, USA, 2020. [CrossRef]
4. Kalogirou, S.A. *Solar Energy Engineering: Processes and Systems*, 2nd ed.; Academic Press: San Diego, CA, USA, 2009. [CrossRef]
5. Santos, D.S.d.O.; de Mattos Neto, P.S.G.; de Oliveira, J.F.L.; Siqueira, H.V.; Barchi, T.M.; Lima, A.R.; Madeiro, F.; Dantas, D.A.P.; Converti, A.; Pereira, A.C.; et al. Solar irradiance forecasting using dynamic ensemble selection. *Appl. Sci.* **2022**, *12*, 3510. [CrossRef]
6. Rajagukguk, R.A.; Ramadhan, R.A.A.; Lee, H.J. A Review on deep learning models for forecasting time series data of solar irradiance and photovoltaic power. *Energies* **2020**, *13*, 6623. [CrossRef]
7. Evans, A.; Strezov, V.; Evans, T.J. Assessment of utility energy storage options for increased renewable energy penetration. *Renew. Sustain. Energy Rev.* **2012**, *16*, 4141–4147. [CrossRef]
8. Wang, Z.; Tuo, X.; Zhou, J.; Xiao, G. Performance study of large capacity industrial lead-carbon battery for energy storage. *J. Energy Storage* **2022**, *55*, 105398. [CrossRef]
9. Bandini, G.; Caposciutti, G.; Marracci, M.; Buffi, A.; Tellini, B. Characterization of lithium-batteries for high power applications. *J. Energy Storage* **2022**, *50*, 104607. [CrossRef]
10. Yanamandra, K.; Pinisetty, D.; Gupta, N. Impact of carbon additives on lead-acid battery electrodes: A review. *Renew. Sustain. Energy Rev.* **2023**, *173*, 113078. [CrossRef]
11. Costa, T.; Vasconcelos, A.; Arcanjo, A.; Silva Junior, W.; Pereira, A.; Jatobá, E.; Filho, J.B.M.; Barreto, E.; Villalba, M.; Marinho, M. PV/BESS microgrid sizing for substation support of the electric power transmission. In *XV SEPOPE—Volume I: Simpósio de Especialistas em Planejamento da Operação e Expansão de Sistemas de Energia Elétrica (Anais de Eventos do CIGRE-Brasil)*; Patriota de Siqueira, I., Ed.; Comitê Nacional Brasileiro de Produção e Transmissão de Energia Elétrica CIGRE-Brasil: Foz do Iguaçu, Brazil, 2022.
12. Yin, J.; Lin, H.; Shi, J.; Lin, Z.; Bao, J.; Wang, Y.; Lin, X.; Qin, Y.; Zhang, W. Lead-carbon batteries toward future energy storage: From mechanism and materials to applications. *Electrochem. Energy Rev.* **2022**, *5*, 3. [CrossRef]
13. Lan, H.; Wen, S.; Hong, Y.Y.; Yu, D.C.; Zhang, L. Optimal sizing of hybrid PV/diesel/battery in ship power system. *Appl. Energy* **2015**, *158*, 26–34. [CrossRef]
14. Yahiaoui, A.; Benmansour, K.; Tadjine, M. Control, analysis and optimization of hybrid PV-Diesel-Battery systems for isolated rural city in Algeria. *Sol. Energy* **2016**, *137*, 1–10. [CrossRef]
15. Liu, C.; Wang, X.; Wu, X.; Guo, J. Economic scheduling model of microgrid considering the lifetime of batteries. *IET Gener. Transm. Distrib.* **2017**, *11*, 759–767. [CrossRef]
16. Sufyan, M.; Abd Rahim, N.; Tan, C.; Muhammad, M.A.; Sheikh Raihan, S.R. Optimal sizing and energy scheduling of isolated microgrid considering the battery lifetime degradation. *PLoS ONE* **2019**, *14*, e0211642. [CrossRef]
17. Chedid, R.; Sawwas, A.; Fares, D. Optimal design of a university campus micro-grid operating under unreliable grid considering PV and battery storage. *Energy* **2020**, *200*, 117510. [CrossRef]
18. Bandyopadhyay, S.; Mouli, G.R.C.; Qin, Z.; Elizondo, L.R.; Bauer, P. Techno-economical model based optimal sizing of PV-battery systems for microgrids. *IEEE Trans. Sustain. Energy* **2020**, *11*, 1657–1668. [CrossRef]
19. Alramlawi, M.; Li, P. Design Optimization of a Residential PV-Battery Microgrid with a Detailed Battery Lifetime Estimation Model. *IEEE Trans. Ind. Appl.* **2020**, *56*, 2020–2030. [CrossRef]
20. Alramlawi, M.; Gabash, A.; Mohagheghi, E.; Li, P. Optimal operation of hybrid PV-battery system considering grid scheduled blackouts and battery lifetime. *Sol. Energy* **2018**, *161*, 125–137. [CrossRef]
21. Zheng, Z.; Li, X.; Pan, J.; Luo, X. A multi-year two-stage stochastic programming model for optimal design and operation of residential photovoltaic-battery systems. *Energy Build.* **2021**, *239*, 110835. [CrossRef]
22. Wu, Y.; Liu, Z.; Liu, J.; Xiao, H.; Liu, R.; Zhang, L. Optimal battery capacity of grid-connected PV-battery systems considering battery degradation. *Renew. Energy* **2022**, *181*, 10–23. [CrossRef]

23. Najafi Ashtiani, M.; Toopshekan, A.; Razi Astaraei, F.; Yousefi, H.; Maleki, A. Techno-economic analysis of a grid-connected PV/battery system using the teaching-learning-based optimization algorithm. *Sol. Energy* **2020**, *203*, 69–82. [CrossRef]

24. Shivam, K.; Tzou, J.C.; Wu, S.C. A multi-objective predictive energy management strategy for residential grid-connected PV-battery hybrid systems based on machine learning technique. *Energy Convers. Manag.* **2021**, *237*, 114103. [CrossRef]

25. Chakir, A.; Tabaa, M.; Moutaouakkil, F.; Medromi, H.; Julien-Salame, M.; Dandache, A.; Alami, K. Optimal energy management for a grid connected PV-battery system. *Energy Rep.* **2020**, *6*, 218–231. [CrossRef]

26. Abushnaf, J.; Rassau, A. Impact of energy management system on the sizing of a grid-connected PV/battery system. *Electr. J.* **2018**, *31*, 58–66. [CrossRef]

27. Mulleriyawage, U.G.K.; Shen, W.X. Optimally sizing of battery energy storage capacity by operational optimization of residential PV-Battery systems: An Australian household case study. *Renew. Energy* **2020**, *160*, 852–864. [CrossRef]

28. Li, J. Optimal sizing of grid-connected photovoltaic battery systems for residential houses in Australia. *Renew. Energy* **2019**, *136*, 1245–1254. [CrossRef]

29. Aziz, A.; Tajuddin, M.; Adzman, M.; Ramli, M.; Mekhilef, S. Energy management and optimization of a PV/diesel/battery hybrid energy system using a combined dispatch strategy. *Sustainability* **2019**, *11*, 683. [CrossRef]

30. Falama, R.Z.; Kaoutoing, M.D.; Mbakop, F.K.; Dumbrava, V.; Makloufi, S.; Djongyang, N.; Salah, C.B.; Doka, S.Y. A comparative study based on a techno-environmental-economic analysis of some hybrid grid-connected systems operating under electricity blackouts: A case study in Cameroon. *Energy Convers. Manag.* **2022**, *251*, 114935. [CrossRef]

31. Alramlawi, M.; Gabash, A.; Mohagheghi, E.; Li, P. Optimal operation of PV-battery-diesel microgrid for industrial loads under grid blackouts. In Proceedings of the 2018 IEEE International Conference on Environment and Electrical Engineering and 2018 IEEE Industrial and Commercial Power Systems Europe (EEEIC/I & CPS Europe), Palermo, Italy, 12–15 June 2018; pp. 1–5. [CrossRef]

32. Hamidieh, M.; Ghassemi, M. Microgrids and resilience: A review. *IEEE Access* **2022**, *10*, 106059–106080. [CrossRef]

33. Liu, Y.; Lei, S.; Hou, Y. Restoration of power distribution systems with multiple data centers as critical loads. *IEEE Trans. Smart Grid* **2019**, *10*, 5294–5307. [CrossRef]

34. Babaei, S.; Jiang, R.; Zhao, C. Distributionally robust distribution network configuration under random contingency. *IEEE Trans. Power Syst.* **2020**, *35*, 3332–3341. [CrossRef]

35. Tabares, A.; Martinez, N.; Ginez, L.; Resende, J.F.; Brito, N.; Franco, J.F. Optimal capacity sizing for the integration of a battery and photovoltaic microgrid to supply auxiliary services in substations under a contingency. *Energies* **2020**, *13*, 6037. [CrossRef]

36. Costa, T.; Arcanjo, A.; Vasconcelos, A.; Silva, W.; Azevedo, C.; Pereira, A.; Jatobá, E.; Filho, J.B.; Barreto, E.; Villalva, M.G.; et al. Development of a method for sizing a hybrid battery energy storage system for application in AC microgrid. *Energies* **2023**, *16*, 1175. [CrossRef]

37. de Araujo Silva Júnior, W.; Vasconcelos, A.; Arcanjo, A.C.; Costa, T.; Nascimento, R.; Pereira, A.; Jatobá, E.; Bione Filho, J.; Barreto, E.; Villalva, M.G.; et al. Characterization of the operation of a BESS with a photovoltaic system as a regular source for the auxiliary systems of a high-voltage substation in Brazil. *Energies* **2023**, *16*, 1012. [CrossRef]

38. Ramos, F.; Pinheiro, A.; Nascimento, R.; Silva Junior, W.D.A.; Mohamed, M.A.; Annuk, A.; Marinho, M.H.N. Development of operation strategy for battery energy storage system into hybrid AC microgrids. *Sustainability* **2022**, *14*, 13765. [CrossRef]

39. ANNEL—Agência Nacional de Energia Elétrica. NOTA TÉCNICA Nº 90/2019–SRT-SCT-SFE/ANEEL. Available online: https://antigo.aneel.gov.br/web/guest/consultas-publicas?p_p_id=participacaopublica_WAR_participacaopublicaportlet&p_p_lifecycle=2&p_p_state=normal&p_p_mode=view&p_p_cacheability=cacheLevelPage&p_p_col_id=column-2&p_p_col_pos=1&p_p_col_count=2&_participacaopublica_WAR_participacaopublicaportlet_ideDocumento=38906&_participacaopublica_WAR_participacaopublicaportlet_tipoFaseReuniao=fase&_participacaopublica_WAR_participacaopublicaportlet_jspPage=%2Fhtml%2Fpp%2Fvisualizar.jsp (accessed on 19 June 2023).

40. ANEEL. Procedimentos de Distribuição de Energia Elétrica no Sistema Elétrico Nacional—PRODIST Modulo 8. 2022. Available online: https://www2.aneel.gov.br/cedoc/aren2021956_2_7.pdf (accessed on 6 June 2023).

41. Silva, T.C.; Pinto, G.M.; de Souza, T.A.Z.; Valerio, V.; Silvério, N.M.; Coronado, C.J.R.; Guardia, E.C. Technical and economical evaluation of the photovoltaic system in Brazilian public buildings: A case study for peak and off-peak hours. *Energy* **2020**, *190*, 116282. [CrossRef]

42. Klein, S.A.; Beckman, W.A.; Mitchell, J.W.; Duffie, J.A.; Duffie, N.A.; Freeman, T.L.; Mitchell, J.C. *TRNSYS 18: A Transient System Simulation Program*; Solar Energy Laboratory, University of Wisconsin: Madison, WI, USA, 2017; Available online: http://sel.me.wisc.edu/trnsys (accessed on 6 June 2023).

43. Mondol, J.D.; Yohanis, Y.G.; Norton, B. Optimising the economic viability of grid-connected photovoltaic systems. *Appl. Energy* **2009**, *86*, 985–999. [CrossRef]

44. Mazzeo, D.; Oliveti, G.; Baglivo, C.; Congedo, P.M. Energy reliability-constrained method for the multi-objective optimization of a photovoltaic-wind hybrid system with battery storage. *Energy* **2018**, *156*, 688–708. [CrossRef]

45. Jiménez-Fernández, S.; Salcedo-Sanz, S.; Gallo-Marazuela, D.; Gómez-Prada, G.; Maellas, J.; Portilla-Figueras, A. Sizing and maintenance visits optimization of a hybrid photovoltaic-hydrogen stand-alone facility using evolutionary algorithms. *Renew. Energy* **2014**, *66*, 402–413. [CrossRef]

46. Blank, J.; Deb, K. Pymoo: Multi-objective optimization in Python. *IEEE Access* **2020**, *8*, 89497–89509. [CrossRef]

47. Regnier, J.; Sareni, B.; Roboam, X. System optimization by multiobjective genetic algorithms and analysis of the coupling between variables, constraints and objectives. *COMPEL—Int. J. Comput. Math.* **2005**, *24*, 805–820. [CrossRef]

48. Petchrompo, S.; Coit, D.W.; Brintrup, A.; Wannakrairot, A.; Parlikad, A.K. A review of Pareto pruning methods for multi-objective optimization. *Comput. Ind. Eng.* **2022**, *167*, 108022. [CrossRef]

49. Ojstersek, R.; Brezocnik, M.; Buchmeister, B. Multi-objective optimization of production scheduling with evolutionary computation: A review. *Int. J. Ind. Eng. Comput.* **2020**, *11*, 359–376. [CrossRef]

50. Deb, K.; Agrawal, S.; Pratap, A.; Meyarivan, T. A fast elitist non-dominated sorting genetic algorithm for multi-objective optimization: NSGA-II. In *International Conference on Parallel Problem Solving from Nature PPSNVI, PPSN: Parallel Problem Solving from Nature*; Lecture Notes in Computer Science; Springer: Berlin/Heidelberg, Germany, 2000; Volume 1917, pp. 849–858. [CrossRef]

51. Shadmand, M.B.; Balog, R.S. Multi-objective optimization and design of photovoltaic-wind hybrid system for community smart DC microgrid. *IEEE Trans. Smart Grid* **2014**, *5*, 2635–2643. [CrossRef]

52. Ghiasi, M. Detailed study, multi-objective optimization, and design of an AC-DC smart microgrid with hybrid renewable energy resources. *Energy* **2019**, *169*, 496–507. [CrossRef]

53. Riou, M.; Dupriez-Robin, F.; Grondin, D.; Le Loup, C.; Benne, M.; Tran, Q.T. Multi-objective optimization of autonomous microgrids with reliability consideration. *Energies* **2021**, *14*, 4466. [CrossRef]

54. Aghajani, G.; Ghadimi, N. Multi-objective energy management in a micro-grid. *Energy Rep.* **2018**, *4*, 218–225. [CrossRef]

55. Zhou, N.; Liu, N.; Zhang, J.; Lei, J. Multi-objective optimal sizing for battery storage of PV-based microgrid with demand response. *Energies* **2016**, *9*, 591. [CrossRef]

56. Chen, J.; Zhang, W.; Li, J.; Zhang, W.; Liu, Y.; Zhao, B.; Zhang, Y. Optimal sizing for grid-tied microgrids with consideration of joint optimization of planning and operation. *IEEE Trans. Sustain. Energy* **2018**, *9*, 237–248. [CrossRef]

57. Huang, Y.; Masrur, H.; Shigenobu, R.; Hemeida, A.M.; Mikhaylov, A.; Senjyu, T. A comparative design of a campus microgrid considering a multi-scenario and multi-objective approach. *Energies* **2021**, *14*, 2853. [CrossRef]

58. MIT. The Future of Energy Storage—An Interdisciplinary MIT Study. 2022. Available online: https://energy.mit.edu/wp-content/uploads/2022/05/The-Future-of-Energy-Storage.pdf (accessed on 6 June 2023).

59. Equatorial Energia Alagoas. Valor de Tarifas e Serviços. Available online: https://al.equatorialenergia.com.br/informacoes-gerais/valor-de-tarifas-e-servicos/#tarifas-grupo-a (accessed on 6 June 2023).